Photocatalytic Oxidation of 2-Propanol on TiO2 Powder and TiO2 Monolayer Catalysts Studied by Solid-State NMR

ARTICLE *in* THE JOURNAL OF PHYSICAL CHEMISTRY B · APRIL 2001

Impact Factor: 3.3 · DOI: 10.1021/jp004381e

Photocatalytic Oxidation of 2-Propanol on TiO_2 Powder and TiO_2 Monolayer Catalysts Studied by Solid-State NMR

Weizong Xu and Daniel Raftery*

H. C. Brown Laboratory, Department of Chemistry, Purdue University, West Lafayette, Indiana 47907-1393

Received: December 6, 2000

The adsorption and photocatalytic oxidation of 2-propanol was studied by solid-state NMR spectroscopy over TiO_2 powder and a TiO_2 monolayer catalyst anchored on porous Vycor glass (TiO_2 /PVG). Two adsorbed 2-propanol species were identified on the TiO_2 powder, a hydrogen-bonded species and a 2-propoxide species, whereas only the H-bonded 2-propanol species was observed on TiO_2/PVG. The photooxidation of 2-propanol proceeded along two parallel routes. The first occurred through the formation of acetone from the H-bonded 2-propanol species and was followed by the aldol condensation of acetone to form mesityl oxide. The subsequent photooxidation of mesityl oxide progressed slowly. Under dark conditions, mesityl oxide and its fragmentation products, acetaldehyde and isobutylene, were found to be in thermal equilibrium. The second route occurred through the relatively rapid and complete oxidation of 2-propoxide to CO_2. In addition, the mobility of H-bonded 2-propanol was found to be important in the photooxidation, particularly when dark regions of the catalyst exist. H-bonded 2-propanol could be converted to 2-propoxide at newly vacated active sites. In contrast, the slow photooxidation rate of 2-propanol to CO_2 on TiO_2/PVG resulted from the availability of only the first, slow reaction route.

1. Introduction

The widespread use of volatile organic compounds (VOC) in both domestic and industrial activity has caused significant environmental problems, such as degraded air quality, contaminated groundwater, global warming, and stratospheric ozone depletion.

Considerable attention has therefore been paid by scientists in recent decades to develop measures to convert these pollutants into nontoxic compounds such as CO_2 and H_2O. Among these detoxification measures, semiconductor photocatalysts, such as TiO_2, ZnO, MgO, and CdS, represent a promising technology due to a number of favorable factors: (1) the photocatalytic oxidation (PCO) can proceed at ambient temperature and pressure; (2) the excitation source can be sunlight or low cost fluorescent lights; and (3) the semiconductor photocatalysts are generally nontoxic, inexpensive, and chemically and physically stable. A number of researchers have reviewed the important features and summarized the research progress on semiconductor photocatalysis at both liquid−solid and gas−solid interfaces.[1,2,3] A number of factors are found to contribute to the complexity of PCO processes, which include the identity, phase, and concentration of contaminants; the morphology and structure of semiconductor catalysts; the type and intensity of the light source; and the oxygen concentration. A complete understanding of the photocatalytic mechanisms is still in its early stages, and thus, a number of detailed studies will be required to improve our understanding of this promising technology.

To explore the reaction mechanisms in heterogeneous photocatalysis, precise identification of the reaction intermediates and in situ monitoring of the evolution of surface species during PCO is important. The majority of studies to date have been carried out under steady-state conditions, and the mechanistic information has been inferred from observed gas-phase intermediates and products, and the reaction kinetics. Some studies were also performed to investigate the adsorbed species on the surface ex situ resulting from PCO by techniques such as temperature-programmed desorption/oxidation (TPD/TPO).[4−7] We have introduced a new in situ approach to study the TiO_2 surface chemistry during PCO, namely solid-state nuclear magnetic resonance (SSNMR) spectroscopy. This technique, which has been applied to numerous heterogeneous thermal catalytic[8] and photocatalytic systems,[9−13] can provide invaluable and complementary structural and dynamic information due to NMR's atomic specificity, high resolution and quantitative capabilities. In particular, SSNMR is well suited to follow the formation and evolution of surface-bound species on the catalysts. In this work, we report in situ observation of surface species evolution during 2-propanol PCO, which provides additional insight into the reaction mechanism.

2-Propanol, along with other alcohols, is a major contaminant in indoor air and air streams.[14−19] It is also an important surface probe for semiconductor metal oxide photocatalytic reactions.[5,6,17,20,21] In addition, because alkanes are believed to oxidize photocatalytically through alcohol intermediates,[22] understanding the alcohol PCO processes should increase the knowledge of alkane PCO as well. The adsorption and decomposition of 2-propanol on TiO_2 has been studied at both the liquid−solid[23−26] and gas−solid interfaces.[4−6,17,18,27−31] Two adsorbed species, molecular 2-propanol and 2-propoxide, were found on the TiO_2 surface.[5,6,27−29] The decomposition of 2-propanol can proceed along two paths by either dehydrogenation or dehydration, and its selectivity strongly depends on the reaction conditions. Under thermal oxidation, acetone, a dehydrogenation product, and propene, a dehydration product, were both detected.[5,21,27,29] In the photooxidation process, however, only acetone was produced, followed by subsequent photooxidation of acetone to produce CO_2 ultimately.[6,18,30,31]

* To whom correspondence should be addressed. E-mail: raftery@purdue.edu

10.1021/jp004381e CCC: $20.00
Published on Web 04/20/2001

However, the mechanism regarding how the adsorbed 2-propanol and 2-propoxide are converted to acetone, and how the formed acetone can be further photooxidized, is still elusive. Bickley[4] proposed formic acid and acetaldehyde as intermediates of subsequent acetone PCO while Rochester[28] suggested the formation of carboxylate species could result. A number of factors affect 2-propanol PCO, including the initial surface coverage of 2-propanol, different adsorption sites of 2-propanol and their behavior during photocatalysis, the formation of acetone and its presence during reaction, the competitive surface adsorption behavior of 2-propanol and acetone during photocatalysis, and a strong oxygen dependence on the rate of PCO.[6,32] In this paper, we report our detailed SSNMR studies of surface species involved in 2-propanol photocatalysis. We evaluate the different activity of molecularly adsorbed 2-propanol versus the chemically adsorbed 2-propoxide species. In addition, new reaction intermediates are identified and as a result, two possible mechanisms will be proposed.

In addition to improving our knowledge about photocatalytic mechanisms, another important driving force is to improve our understanding regarding the factors that allow the enhancement of the oxidation efficiency through modification of the catalyst itself. Generally, a thin film of catalyst particles are physically coated over a support, such as alumina foam,[33] paper,[34] fiberglass cloth,[35] fused-silica glass fibers,[19] optical microfibers,[12,13] tungsten mesh,[36−39] or ceramic honeycomb monoliths.[4,40] Much attention has also been paid to the chemical modification of support materials, such as porous Vycor glass (PVG), where one or more layers of TiO_2 can be anchored. This could be done by the reaction of $TiCl_4$ with surface OH groups[41−44] or, recently, by metal ion-implantation.[45] One of the advantages of chemical modification is that the surface coverage or content of the photocatalyst can be completely controlled through synthesis. Furthermore, it has been demonstrated that for some reactions the photocatalytic activity was higher in thin film photocatalysts than that for the TiO_2 powder, such as in the reaction of C_3H_4 with water,[41] reduction of CO_2,[46] degradation of 1-octanol[43] and acetone.[47,48] In this paper, we will compare the 2-propanol photocatalytic behavior on TiO_2 powder and a TiO_2 monolayer catalyst anchored on porous Vycor glass (TiO_2/PVG). NMR studies give insight as to several of the factors that influence the photocatalytic behavior.

2. Experiment

2.1. Catalyst Preparation. Photocatalytic oxidation reactions were performed under batch conditions at room temperature using samples sealed in glass NMR tubes. Our procedure for preparing catalyst samples of TiO_2 powder (Degussa P-25, approximately 70% anatase and 30% rutile, BET surface area 55 $m^2\ g^{-1}$), and TiO_2/PVG have been described in detail by Hwang et al.[10,13] Briefly, approximately 170 mg TiO_2 powder was packed into a 5 mm glass NMR tube (Norell), which was then attached to a gas manifold. The powder was first evacuated at 773 K in a ceramic heater for 4 h to remove the adsorbed species and then calcined at 773 K for another 4 h under 1 atm of O_2. The powder was then evacuated to 5×10^{-5} Torr, allowed to cool to room temperature in preparation for loading 2-propanol.

A monolayer TiO_2/PVG catalyst was prepared using the hydrolysis of gas-phase $TiCl_4$ with OH groups on the PVG surface.[41−43] A 3.6 mm diameter PVG rod (Corning 7930, BET surface area $\approx$ 150 m^2/g, pore diameter 40 Å) was fitted into a 5 mm glass NMR tube (Norell). The PVG rod weighed approximately 170 mg and was 12 mm in length. The glass NMR tube was then attached to a gas manifold and the PVG rod was degassed and calcined for 4 h each. To ensure the formation of a complete TiO_2 layer, the calcined PVG rod underwent a series of four reaction cycles with 88 μmol $TiCl_4$ (Aldrich), which was introduced by gas-phase adsorption. The HCl produced in this reaction was evacuated after each cycle. Once the TiO_2 was anchored to the PVG, the catalyst was hydrated, degassed and calcined for 4 h under 1 atm of O_2 at 773 K. The TiO_2/PVG catalyst was then evacuated to 5×10^{-5} Torr and allowed to cool to room temperature before loading with reagents.

TABLE 1: Sample Coverage Evaluation on TiO_2 Powder

sample	total loading μmol	gas phase (%)	surface coverage (monolayer)
SI	16	0.2	0.52
SII	32	0.4	1.0
SIII	48	0.8	1.6
SIV	64	1.0	2.1
SV	128	2.3	4.1

2.2. Sample Preparation. Central-carbon labeled 2-propanol ($CH_3{}^{13}CHOHCH_3$, Cambridge Isotope) was loaded onto the previously calcined catalysts at room temperature using a gas manifold. Five different quantities of 2-propanol, 16, 32, 48, 64 or 128 μmol, were used in this study, the first four of which were loaded onto the TiO_2 powder catalyst along with 90 μmol O_2. The sample with 128 μmol of 2-propanol contained 16 μmol of O_2. To evaluate the surface coverage, a BET analysis of 2-propanol adsorbed on the TiO_2 powder was performed, and a one-monolayer coverage of 2-propanol was found to correspond to 2.0 molecules/nm^2 on the TiO_2 (Degussa P25) powder. This result is comparable to the value of 2.51 molecules/nm^2 on 100% anatase catalyst measured gravimetrically in a high-vacuum system.[5] The previously reported saturation coverage[6] (4.2 molecules/nm^2) of 2-propanol on the Degussa powder, which was measured by TPD (temperature-programmed decomposition) in an annular reactor, could include a physisorbed layer of 2-propanol as well. According to our BET data, a one-monolayer coverage of 2-propanol corresponds to 31 μmol for 170 mg of Degussa TiO_2 powder. A calibration curve of gas-phase pressure versus total loading of 2-propanol was also made to evaluate the percentage of gas phase 2-propanol at each sample loading. Because the dead volume of the NMR tube is very small ($\sim$0.3 mL), the amount of 2-propanol in the gas phase is limited to a maximum of 0.7 μmol at its saturated vapor pressure, 45 Torr at 298 K. Therefore the gas-phase content is limited to less than 3% of the total 2-propanol in each sample. The sample loadings, evaluation of the gas-phase percentages, and surface coverages for each of the five TiO_2 powder samples (SI−SV) are listed in Table 1.

Another sample (sample SVI) was prepared by loading 40 μmol of 2-propanol, which corresponds to a $^1/_2$ monolayer coverage, on the TiO_2/PVG catalyst, along with 90 μmol of O_2. The coverage calculation is based on the surface area of PVG (150 m^2/g). After sample loading, all glass NMR tubes were flame sealed 10−12 mm above the catalyst samples.

2.3. In Situ SSNMR Methods. A home-built magic angle spinning (MAS) probe and light delivery system was used for in situ photocatalytic studies.[10] A 300 W Xe−Arc lamp (ILC) was used as the UV source. Light in the range of 350 to 450 nm was selected using a dichroic mirror (Oriel Corp.). The near-UV light was delivered to the sample located inside the NMR magnet using a liquid-filled optical light guide (Oriel Corp.). The MAS probe was doubly tuned for ^{1}H and ^{13}C observation at frequencies of 300 and 75.4 MHz, respectively, and was

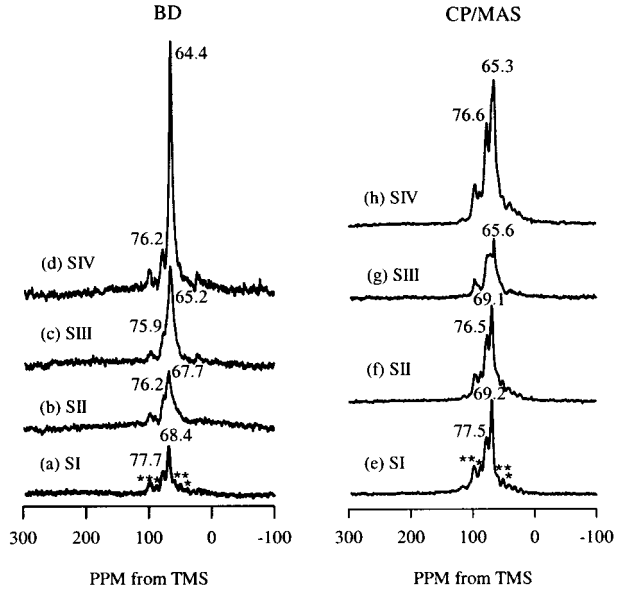

Figure 1. Proton-decoupled ^{13}C MAS Bloch decay (BD) and corresponding CP/MAS NMR spectra at different surface coverages of 2-propanol on TiO_2 powder before irradiation. (a) BD, sample SI (0.52 monolayer coverage); (b) BD, sample SII (1.0); (c) BD, sample SIII (1.6); (d) BD, sample SIV (2.1); (e) CP/MAS, sample SI; (f) CP/MAS, sample SII; (g) CP/MAS, sample SIII; and (h) CP/MAS, sample SIV. Each spectrum consists of the average of 200 transients with 8 s recycle delay time. The CP/MAS spectra were obtained using a 50 μs contact time. The asterisks indicate spinning sidebands of surface bound species.

capable of spinning the sealed samples up to 2.7 kHz. The near UV light power irradiating the sample was measured to be 5 mW.

3. Results and Discussion

3.1. Adsorption of 2-Propanol. The adsorption of 2-propanol on the TiO_2 powder and TiO_2/PVG catalysts was examined using proton-decoupled ^{13}C MAS Bloch Decay (BD) and corresponding CP/MAS NMR methods. By comparing BD and CP/MAS spectra, the relative mobility of different species can be evaluated because the signal intensity of CP/MAS spectrum is inversely related to the mobility. Although CP/MAS spectra can be somewhat nonquantitative, in conjunction with quantitative BD, CP/MAS NMR can be a very useful assignment tool for surface analysis.

TiO_2 Powder Catalyst. The proton-decoupled ^{13}C BD and corresponding CP/MAS NMR spectra of TiO_2 powder samples SI, SII, SIII, and SIV before irradiation are shown in Figure 1. It has been reported that 2-propanol adsorbed on TiO_2 surface can be present in two forms: a hydrogen-bonded physisorbed species and a chemisorbed 2-propoxide species.[5,6,27−29] In our sealed samples, a small percentage of gas phase 2-propanol is present as well, and the contribution of the gas-phase 2-propanol in each sample is listed in Table 1. The peak at 64.4 ppm corresponds to 2-propanol, and contains contributions primarily from H-bonded 2-propanol, as well as a small percentage of gas-phase molecules. Gas-phase and weakly surface-bound 2-propanol exchange rapidly since no unique resonance is observed for the gas-phase species. As shown in the BD spectra in Figure 1a through Figure 1d, the chemical shift of H-bonded/gas phase 2-propanol changes as a function of surface coverage. The chemical shift of H-bonded species decreases from 68.4 ppm in SI, to 67.7 ppm in SII, 65.2 ppm in SIII, and finally to 64.4 ppm in SIV. The chemical shift in sample SIV is approximately the same as the liquid-phase chemical shift of

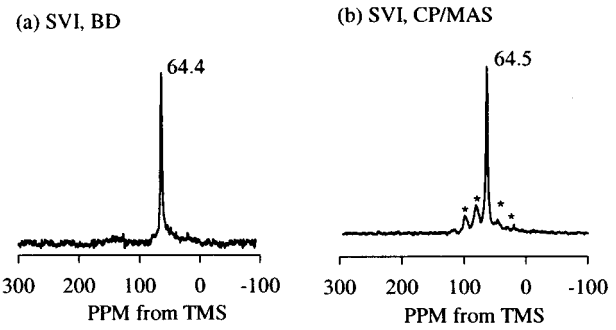

Figure 2. Proton-decoupled ^{13}C MAS BD and corresponding CP/MAS NMR spectra of 2-propanol adsorbed on TiO_2/PVG (sample SVI: $^1/_2$ monolayer coverage): (a) BD; (b) CP/MAS.

64.2 ppm for neat 2-propanol.[49] We assign the peak near 76 ppm to the 2-propoxide species, which parallels our NMR observations of the adsorption of ethanol.[11,13] The chemical shift of the 2-propoxide species changes from 77.7 ppm in SI, to 76.2 ppm in SII and then is relatively constant after a one monolayer surface coverage is reached as shown by the measured chemical shifts of 75.9 ppm in SIII and 76.2 ppm in SIV. The BD spectrum (not shown) of sample SV simply shows an increase in the peak intensity at 64.4 ppm over that of sample SIV due to the large increase in concentration of physisorbed 2-propanol as indicated in Table 1.

To examine species with restricted mobility, CP/MAS spectra were collected using a short contact time of 50 μs. As shown in Figure 1e−h, the chemical shifts for these strongly bound species follow a similar trend to that observed in the corresponding BD spectra. However, the chemical shifts observed in the CP/MAS spectra are a bit larger than those in the corresponding BD spectra because the CP technique favors those species that are more strongly bound. The variation of chemical shifts at different surface coverages indicates the formation of different adsorption sites**,** and is evident in Fig 1, parts g and h. The chemical shift of the H-bonded species changes from 69.1 ppm (SII) to 65.6 ppm (SIII), whereas the chemical shift of 2-propoxide shows a broad range, indicating a heterogeneous distribution of 2-propoxide sites. The formation of multiple ethoxide species upon the adsorption of ethanol on TiO_2 powder was also observed at different sites.[13] As the coverage increases, there is a possibility for an increase in the mobility and/or exchangeability of species among the different adsorption sites (vida infra). The effect of this mobility on the photooxidation will be evaluated below.

PVG/TiO_2 Catalyst. The proton-decoupled ^{13}C BD and corresponding CP/MAS NMR spectra of sample SVI before irradiation are shown in Figure 2. As shown, only one peak was observed in both the BD and the CP/MAS NMR spectra on the TiO_2/PVG surface. The peak at 64.4 ppm in the BD can be ascribed to mobile species, including weakly H-bonded and gas-phase 2-propanol species. The peak at 64.5 ppm in the CP/MAS spectrum, along with its associated sidebands, indicates the presence of species with restricted mobility, that is, strong hydrogen bonding as well. However, the formation of 2-propoxide is not observed on the TiO_2/PVG as it was on the TiO_2 powder at the same coverage (sample SI). This result is also in contrast to the formation of the ethoxide species on TiO_2/PVG.[11,13] This unusual behavior for 2-propanol adsorption on TiO_2/PVG may result from a molecular-scale steric effect of 2-propanol[5] and a relatively weak H-bonding strength between 2-propanol and the surface. The adsorption behavior of different alcohols on TiO_2 powder has been previously investigated.[5] It was found that the concentration of alkoxide species was less

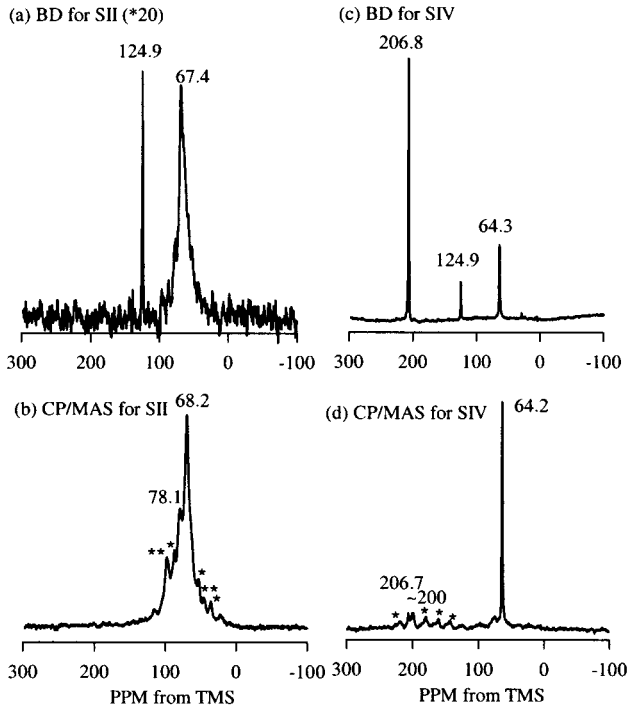

Figure 3. Proton-decoupled ^{13}C MAS BD NMR of 2-propanol on TiO_2 powder after 3 h in situ irradiation of sample SII and sample SIV. (a) BD, sample SII; (b) CP/MAS, sample SII. A contact time of 50 μs was applied. (c) BD, sample SIV; (d) CP/MAS, sample SIV. A contact time of 2500 μs was applied.

for secondary alcohols (e.g., 2-propanol) than that for the primary alcohols (e.g., ethanol) due to a steric effect based on the relative size of the adsorbate and the coordinatively unsaturated Ti active site. Apparently, the H-bonding of 2-propanol is not strong enough to form its dehydration product, 2-propoxide, on TiO_2/PVG. In the TiO_2 powder surface, however, the presence of defect sites, such as those found at particle edges, and a denser surface concentration of OH groups make the formation of 2-propoxide possible.[5] In the present study, the simple nature of 2-propanol adsorption on TiO_2/PVG catalyst makes it feasible to evaluate the mechanism of the photooxidation of 2-propanol by isolating the effect of the H-bonded 2-propanol species.

3.2. Photocatalytic Oxidation of 2-Propanol. *TiO_2 Powder Catalyst*. Proton-decoupled ^{13}C BD NMR and corresponding CP/MAS spectra of samples SII and SIV are shown in Figure 3 after 3 h of in situ irradiation. For SII, CO_2 is produced within 1 h of in situ irradiation and its presence is very apparent at 124.9 ppm in the BD spectrum after 3 h of in situ irradiation (Figure 3a). By comparing the CP/MAS spectra before (Figure 1f) and after (Figure 3b) in situ irradiation, a large decrease in intensity of the 2-propoxide over that of the H-bonded species is evident. This indicates that the chemisorbed 2-propoxide species is more reactive than the physisorbed 2-propanol species, a result that parallels our findings for ethanol.[11,13] By comparison, the photooxidation of sample SIV results in acetone formation (206.8 ppm) immediately following in situ irradiation, in addition to the formation of CO_2 (124.9 ppm). The narrow line widths of the acetone and CO_2 peaks indicate that the produced acetone and CO_2 are weakly adsorbed on the surface. As shown in the BD spectrum (Figure 3c), after 3 h in situ irradiation the 2-propoxide species reacts almost to completion, whereas significant amounts of 2-propanol remain. Because the oxidation of acetone to CO_2 on TiO_2 powder was very slow and the complete oxidation product (CO_2) from acetone was observed in FTIR experiments only under conditions of high oxygen concentration,[50,51] the formation of CO_2 in this experiment should occur directly through the decomposition of 2-propoxide. We therefore find that the decomposition of 2-propoxide is more effective than that of 2-propanol itself. A similar behavior was also reported by Muggli et al.[52] for ethanol, in that the H-bonded ethanol species preferentially oxidized to acetaldehyde, whereas the ethoxide preferentially oxidized completely to CO_2. To investigate the more weakly bound surface species, a long contact time (2500 μs) CP/MAS experiment was performed, and the corresponding spectrum is shown in Figure 3d. Mesityl oxide, the product of acetone aldol condensation is observed at ~200 ppm in addition to the weakly adsorbed acetone species at 206.7 ppm. The aldol condensation of acetone will be discussed further in reference to the PVG/TiO_2 surface.

By comparing the photocatalytic behavior of samples SII and SIV, it is apparent that the H-bonded 2-propanol is oxidized immediately to acetone in sample SIV, whereas 2-propanol remains in sample SII after in situ irradiation. This can be ascribed to their different mobilities in these samples. As shown in Figure 1b, the H-bonded 2-propanol in sample SII with a one-monolayer coverage has limited mobility, which is indicated by its broad peak and the offset of its chemical shift (67.7 ppm) from that of liquid-state 2-propanol (64.2 ppm). In sample SIV, however, the surface coverage is roughly 2 monolayers. The H-bonded 2-propanol in the second physisorbed monolayer is quite mobile, as indicated by its intense, narrow peak and the chemical shift (64.4 ppm). In our experimental setup, only a small fraction of the packed powdered TiO_2 surface can be irradiated by UV light. The ineffective photocatalytic conversion of immobile 2-propanol in SII indicates that most of these species are located in dark areas of the catalyst that are not accessible to UV light. Therefore, no visible acetone formation is observed in SII. As to the 2-propanol species in SIV, however, its increased mobility can aid its photocatalytic oxidation since it can migrate to the illuminated area, and therefore be photooxidized to acetone as observed. To confirm this statement, a PCO experiment of 2-propanol with less than a one-monolayer coverage was conducted using FTIR detection.[50] We sprayed TiO_2 powder on a tungsten mesh support such that a thin film of TiO_2 was evenly distributed on the mesh, and could be illuminated evenly. In comparison to TiO_2 powder packed into a 5 mm glass NMR tube, this method should create a much more homogeneously irradiated catalyst. In this experiment, which will be reported in detail at a later date, the formation of acetone (and CO_2) was observed rapidly after initiating UV irradiation.

We also observe that the amount of CO_2 formed in SIV is roughly 3 times that in sample SII after 3 h in situ irradiation, and the decomposition of 2-propanol is about 70% in sample SIV compared with 40% in sample SII. The faster oxidation rate of 2-propanol in sample SIV indicates that its mobility accelerates the PCO process. The rapid formation of CO_2 in SIV also indicates that the H-bonded 2-propanol can migrate to vacant active sites where it converts to 2-propoxide and then can be converted quickly to CO_2 under UV irradiation. The chemical shifts of different species observed during PCO are listed in Table 2. A proposed mechanism for 2-propanol photooxidation on TiO_2 powder is shown in Figure 4.

PVG/TiO_2 Catalyst. Photocatalytic oxidation of 2-propanol on TiO_2/PVG was examined using different irradiation time periods, as shown in Figure 5 for BD spectra and Figure 6 for the CP/MAS NMR spectra. As reported above, only one peak

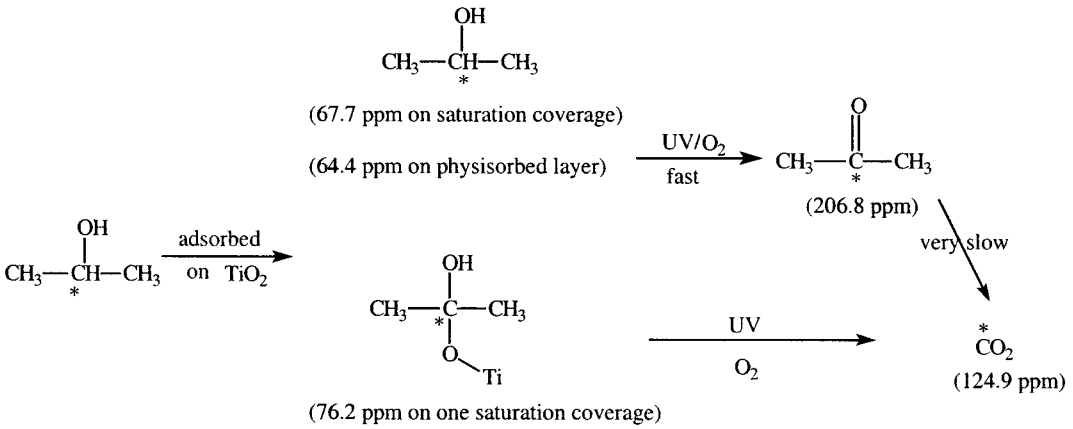

Figure 4. Proposed mechanism for 2-propanol photooxidation on TiO_2 powder. Asterisks indicate ^{13}C nuclei.

TABLE 2: Chemical Shifts of Different Species on TiO_2 Powder and TiO_2/PVG

catalyst	species	chemical shift (ppm)
TiO_2 powder	2-propanol	64.4
	2-propoxide	76.2
	acetone	206.8
	CO_2	124.9
TiO_2/PVG	2-propanol	64.4
	acetone	212
	mesityl oxide	205; 160[51,52]
acetaldehyde	198	
isobutylene	140	
acetic acid	180	

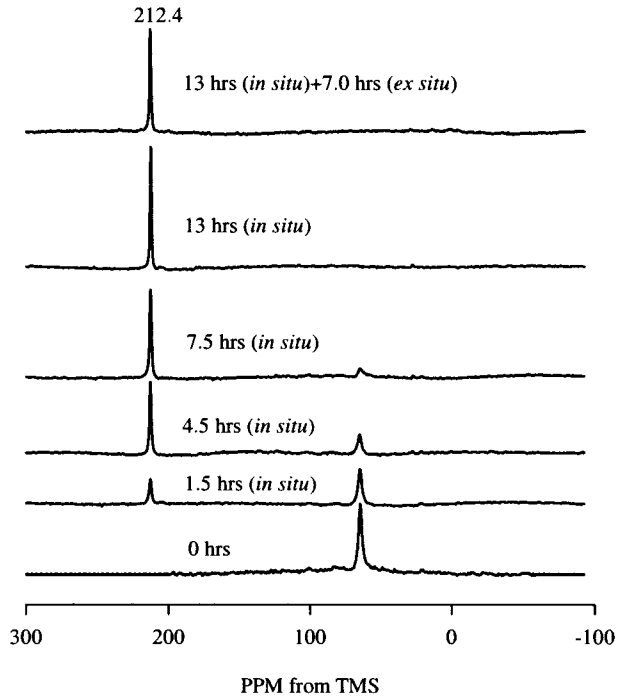

Figure 5. Proton-decoupled ^{13}C MAS BD NMR spectra of 2-propanol on TiO_2/PVG during photocatalytic oxidation. Irradiation times are noted as shown.

at 64.4 ppm, assigned to the H-bonded 2-propanol species, was observed for the TiO_2/PVG sample. The narrow line width of the peak associated with this species indicates its high mobility. As the sample was irradiated, acetone (212.4 ppm) was produced rapidly. Acetone remained very weakly adsorbed as indicated by its narrow line width. The exclusive formation of the H-bonded 2-propanol species on PVG/TiO_2 can help evaluate its effect on the photooxidation process without complications

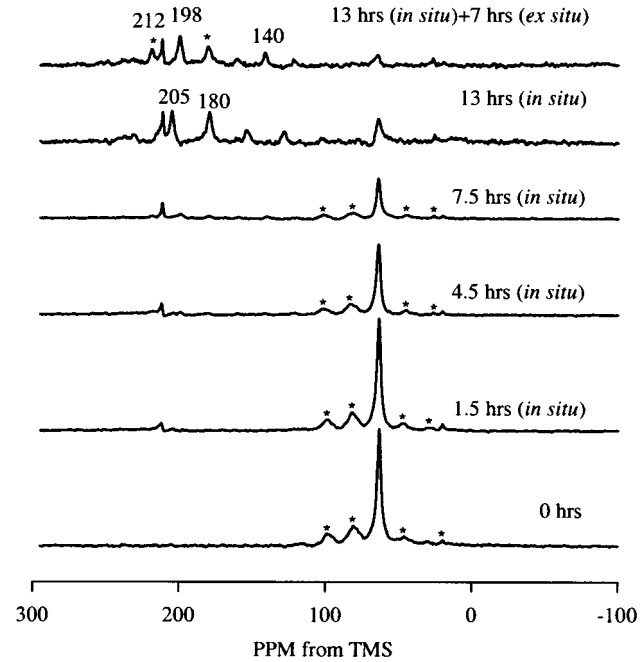

Figure 6. Proton-decoupled ^{13}C CP/MAS NMR spectra of 2-propanol on TiO_2/PVG during photocatalytic oxidation. The asterisks indicate spinning sidebands of surface bound species.

due to the presence of chemisorbed 2-propoxide. As shown in Figure 5, the only change observed in BD spectra is the conversion of 2-propanol to acetone at 212.4 ppm. After the complete conversion of 2-propanol to acetone proceeded after 13 h of in situ irradiation, further ex situ irradiation (7.0 h) did not change the BD spectra significantly.

CP/MAS NMR spectra of this sample provide further information on the surface reactions. A peak was observed at ~205 ppm and corresponds to the aldol condensation species (mesityl oxide)[49] of acetone. This species was only distinguishable after complete conversion of 2-propanol using 13 h of in situ irradiation. Mesityl oxide was weakly adsorbed on the surface according to the CP/MAS spectra. To observe this weakly adsorbed species, a longer contact time of 2500 μs was necessary. The expected quaternary ^{13}C peak at 160 ppm was invisible using CP/MAS due to the lack of the attached proton and its weak adsorption.[53] Luo and Falconer[54] reported and compared the extent of the aldol condensation of acetone on different TiO_2 powder morphologies. El-Maazawi et al.[51] recently reported their observations of aldol condensation of acetone on Degaussa TiO_2 powder and measured the dependence of aldol condensation on the surface coverage using FTIR

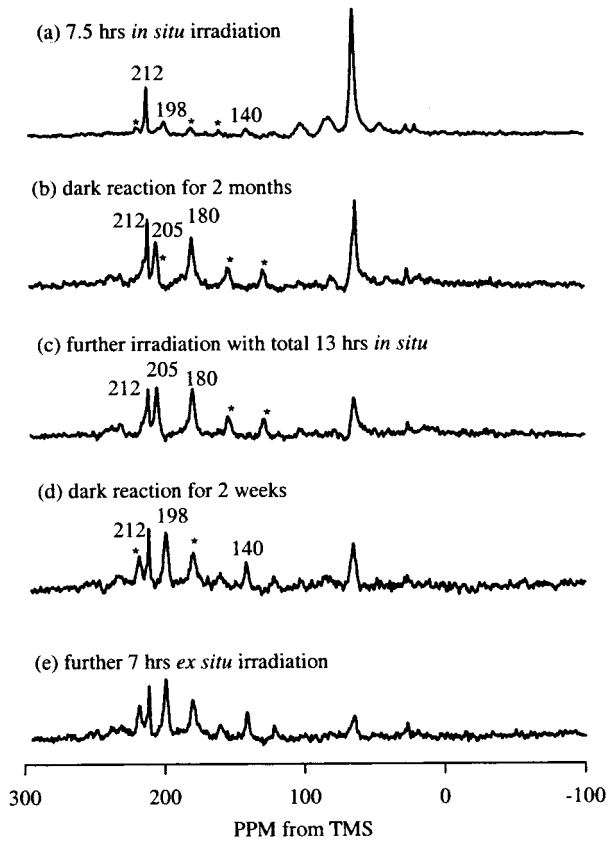

Figure 7. Comparison of proton-decoupled ^{13}C CP/MAS NMR spectra of 2-propanol on TiO_2/PVG before and after dark reactions and further irradiation: (a) spectrum obtained after 7.5 h of in situ irradiation; (b) spectrum obtained after sample was placed in the dark for 2 months; (c) sample irradiated in situ for a total of 13 h; (d) sample placed in the dark for 2 weeks following (c); and (e) sample further irradiated in situ for a total of 13 h plus 7 h of ex situ irradiation following (d).

methods. The aldol condensation of acetone on TiO_2/PVG has not yet been reported to the best of our knowledge. As the studies of acetone adsorbed on zeolites[53] and other metal oxides[55] have shown, the reaction of acetone could yield different products through aldol condensation and secondary reactions such as double bond migration, hydride transfer, and cracking. The extent of reaction and the selectivity for various products depended on the surface acidity of the metal oxides and the reaction conditions. The aldol condensation of acetone was also observed in CsX and CsY catalysts with weak acidity comparable to acetic acid. Because the TiO_2/PVG surface only demonstrates weak surface acidity, condensation can be predicted to occur slowly. As the irradiation continued, the mesityl oxide broke up into smaller fragments. Acetaldehyde at ~198 ppm and isobutylene at ~140 ppm were observed and were relatively strongly adsorbed onto the surface according to the peak widths and spinning sidebands evident in the CP/MAS spectra.

Interestingly, the mesityl oxide surface species could evolve in the dark. This was indicated by the disappearance of peaks at 198 and 140 ppm and the appearance of peaks at 205 and 180 ppm after the sample was placed in the dark for a period of two months following 7.5 h in situ irradiation (Figure 7a, 7b). The reappearance of the peak at 205 ppm indicated the reversible thermal fragmentation of the mesityl oxide. The appearance of the peak at 180 ppm indicated the partial thermal oxidation of acetaldehyde to acetic acid, which was also strongly adsorbed on the surface. Note that the peak at 205 ppm in Figure 7b was buried in the sidebands of acetic acid, and the confirmation of this species can be indicated by its peak becoming stronger than that of the peak at 180 ppm after further irradiation of the sample in Figure 7c. The reversible thermal fragmentation of mesityl oxide was further confirmed by observing the NMR spectrum following 13 h irradiation and an additional 2 week period in the dark (Figure 7c and 7d). The peak at 205 ppm has disappeared, whereas the reappearance of peaks at 198 and 140 peaks is again evident in the Figure 7d. Further UV irradiation only increased the ratio of product in the favored direction as shown in Figure 7, parts c and e, as compared with Figure 7, parts b and d. As the result of this reversible reaction, the photooxidation of 2-propanol on TiO_2/PVG was not complete and CO_2 was never observed, even after a total 20 h of UV irradiation. The chemical shifts of different species during PCO are listed in Table 2. The proposed mechanism for 2-propanol photooxidation on TiO_2/PVG is shown in Figure 8.

Conclusions

Photocatalytic reactions of 2-propanol on TiO_2 powder and TiO_2/PVG have been examined using in situ SSNMR detection methods. The following conclusions can be derived from the above discussions:

(1) H-bonded 2-propanol and 2-propoxide species were found on TiO_2 powder upon adsorption of 2-propanol, whereas only the H-bonded species were found on the TiO_2/PVG sample. On TiO_2 powder, 2-propoxide has multiple adsorption sites that were observed at low coverage. At coverages above one monolayer, H-bonded 2-propanol with increasing mobility was observed.

(2) The photooxidation of 2-propanol could proceed through two parallel routes. The first route occurred through the formation of acetone from the H-bonded 2-propanol species and was followed by the aldol condensation of acetone to form

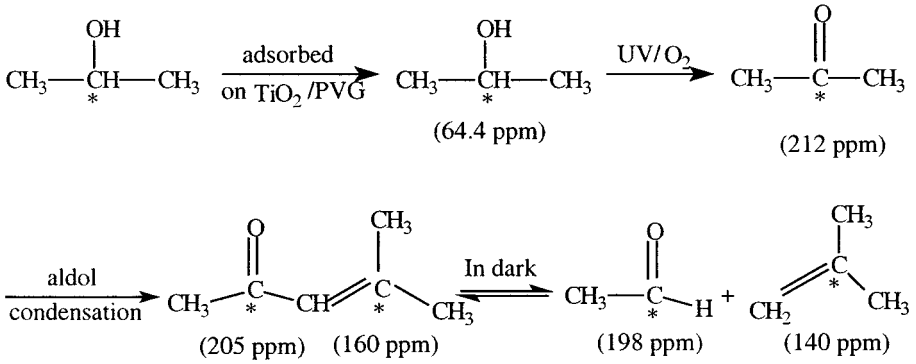

Figure 8. Proposed mechanism for 2-propanol photooxidation on TiO_2/PVG.

mesityl oxide. The subsequent photooxidation of mesityl oxide progressed slowly. Under dark conditions, mesityl oxide and its fragmentation products, acetaldehyde and isobutylene, were found to be in thermal equilibrium. The second route occurred through the relatively rapid oxidation of the 2-propoxide species to form CO_2 directly.

(3) The mobility of the H-bonded species is important for 2-propanol PCO as it can improve the photoactivity, particularly when such species are located in dark regions of the catalyst. Mobile 2-propanol migrates to unoccupied, strong binding sites where it can be converted to the more reactive 2-propoxide species.

(4) On TiO_2/PVG, the lack of 2-propoxide formation made only the first photooxidation route possible and resulted in its very slow oxidation rate to CO_2.

Acknowledgment. The authors thank the NSF (Grant No. CHE-97-33188, CAREER Grant) and the donors of Petroleum Research Fund, administered by the American Chemical Society for funding this work. W.X. thanks Purdue's Environmental Science and Engineering Institute for a graduate fellowship. D.R. is an A.P. Sloan Foundation Fellow (1999-2001).

References and Notes

(1) Hoffmann, M. R.; Martin, S. T.; Choi, W.; Bahnemann, D. W. *Chem. Rev.* **1995**, *95*, 69.
(2) Fox, M. A.; Dulay, M. T. *Chem. Rev.* **1993**, *93*, 341.
(3) Linsebigler, A. L.; Lu, G. Q.; Yates, J. T. *Chem. Rev.* **1995**, *95*, 735.
(4) Bickley, R. I.; Jayanty, R. K. M. *Faraday Discuss. Chem. Soc.* **1974**, *58*, 194.
(5) Kim, K. S.; Barteau, M. A.; Farneth, W. E. *Langmuir* **1988**, *4*, 533.
(6) Larson, S. A.; Widegren, J. A.; Falconer, J. L. *J. Catal.* **1995**, *157*, 611.
(7) Lu, G. Q.; Linsebigler, A.; Yates, J. T. *J. Phys. Chem.* **1995**, *99*, 7626.
(8) Haw, J. F.; Nicholas, J. B.; Xu, T.; Berk, L. W.; Ferguson, D. B. *Acc. Chem. Res.* **1996**, *29*, 259.
(9) Hwang, S−J.; Petucci, C.; Raftery, D. *J. Am. Chem. Soc.* **1997**, *119*, 7877.
(10) Hwang, S−J.; Petucci, C.; Raftery, D. *J. Am. Chem. Soc.* **1998**, *120*, 4388.
(11) Hwang, S−J.; Raftery, D. *Catal. Today* **1999**, *1579*, 1.
(12) Rice, C. V.; Raftery, D. *Chem. Commun.* **1999**, 1.
(13) Pilkenton, S.; Hwang, S−J.; Raftery, D. *J. Phys. Chem. B* **2000**, *103*, 11 152.
(14) Peral, J.; Ollis, D. *J. Catal.* **1992**, *136*, 554.
(15) Jacoby, W. A.; Blake, D. M.; Fennell, J. A. *J. Air Waste Manage. Assoc.* **1996**, *46*, 891.
(16) Alberici, R. M.; Jardim, W. F. *Appl. Catal. B: Environ.* **1997**, *14*, 55.
(17) Ohko, Y.; Hashimoto, K.; Fujishima, A. *J. Phys. Chem. A* **1997**, *101*, 8057.
(18) Ohko, Y.; Fujishima, A.; Hashimoto, K. *J. Phys. Chem. B* **1998**, *102*, 1724.
(19) Hager, S.; Bauer, R. *Chemosphere* **1999**, *38*, 1549.
(20) Raupp, G. B.; Junio, C. T. *Appl. Surf. Sci.* **1993**, *72*, 321.
(21) Rekoske, J. E.; Barteau, M. A. *J. Catal.* **1997**, *165*, 5772.
(22) Djeghri, N.; Teichner, S. J. *J. Catal.* **1980**, *62*, 99.
(23) Harbour, J. R.; Hair, M. L. *J. Phys. Chem.* **1977**, *81*, 1791.
(24) Harvey, P. R.; Rudham, R.; Ward, S. *J. Chem. Soc., Faraday Trans. 1* **1983**, *79*, 2975.
(25) Harvey, P. R.; Rudham, R.; Ward, S. *J. Chem. Soc., Faraday Trans. 1* **1983**, *79*, 1381.
(26) Green, K. J.; Rudham, R. *J. Chem. Soc., Faraday Trans.* **1992**, *88*, 3599.
(27) Nakajima, T.; Miyata, H.; Kobokawa, Y. *Bull. Chem. Soc. Jpn.* **1982**, *55*, 609.
(28) Rochester, C. H.; Graham, J.; Rudham, R. *J. Chem. Soc., Faraday Trans. 1* **1984**, *80*, 2459.
(29) Hussein, G. A. M.; Sheppard, N.; Zaki, M. I.; Fahim, R. B. *J. Chem. Soc., Faraday Trans. 1* **1989**, *85*, 1723.
(30) Brinkley, D.; Engel, T. *Surf. Sci.* **1998**, *415*, L1001.
(31) Brinkley, D.; Engel, T. *J. Phys. Chem. B.* **1998**, *102*, 7596.
(32) Bickley, R. I.; Munuera, G.; Stone, F. S. *J. Catal.* **1973**, *31*, 398.
(33) Nimlos, M. R.; Jacoby, W. A.; Blake, D. M.; Mline, T. A. *Environ. Sci. Technol.* **1993**, *27*, 732.
(34) Matsubara, H.; Takada, M.; Koyama, S.; Hashimoto, K.; Fujishima, A. *Chem. Lett.* **1995**, 767.
(35) Chen, S.; Cheng, X.; Tao, Y.; Zhao, M. *J, Chem, Technol. Biotechnol.* **1998**, *73*, 264.
(36) Wong, J. C. S.; Linsebigler, A.; Lu, G. Q.; Fan, J. F.; Yates, J. T. *J. Phys. Chem.* **1995**, *99*, 335.
(37) Fan, J. F.; Yates, J. T. *J. Am. Chem. Soc.* **1996**, *118*, 4686.
(38) Driessen, M. D.; Goodman, A. L.; Miller, T. M.; Zaharias, G. A.; Grassian, V. H. *J. Phys. Chem. B* **1998**, *102*, 549.
(39) Miller, M. L.; Borisch, J.; Raftery, D.; Francisco, J. S. *J. Am. Chem. Soc.* **1998**, *120*, 8265.
(40) Sauer, M. L.; Ollis, D. F. *J. Catal.* **1998**, *149*, 81.
(41) Anpo, M.; Aikawa, N.; Kubokawa, Y. *J. Phys. Chem.* **1985**, *89*, 5017.
(42) Anpo, M.; Sunamoto, M.; Che, M. *J. Phys. Chem.* **1989**, *93*, 1187.
(43) Yamashita, H.; Ichihashi, Y.; Harada, M.; Steward, G.; Fox, M. A.; Anpo, M. *J. Catal.* **1996**, *158*, 97.
(44) Kawamura, H.; Okuto, S.; Taruta, S.; Takusagawa, N.; Kitajima, K. *J. Ceram. Soc. Jpn.* **1996**, *104*, 1160.
(45) Yamashita, H.; Honda, M.; Harada, M.; Ichihashi, Y.; Anpo M. *J. Phys. Chem. B* **1998**, *102*, 10 707.
(46) Anpo, M.; Chiba, K. *J. Mol. Catal.* **1992**, *74*, 207.
(47) Yu, J.; Lin, J.; Kwok, R. W. M. *J. Photochem. Photobiol. A: Chem.* **1997**, *111*, 199.
(48) Xu, W.; Raftery, D., in preparation.
(49) *Sadtler Standard Carbon-13 NMR spectra*; Bio-Rad Laboratories: Philadelphia, PA, 1994.
(50) Xu, W.; Raftery, D.; Francisco, J., in preparation.
(51) El-Maazawi, M.; Finken, A. N.; Nair, A. B.; Grassian, V. H. *J. Catal.* **2000**, *191*, 138.
(52) Muggli, D. S.; Lowery, K. H.; Falconer, J. L. *J. Catal.* **1998**, *180*, 111.
(53) Xu, T.; Munson, E. J.; Haw, J. F. *J. Am. Chem. Soc.* **1994**, *116*, 1962.
(54) Luo, S.; Falconer, J. L. *J. Catal.* **1999**, *185*, 393.
(55) Zaki, M. I.; Hasan, M. A.; Al-Sagheer, F. A.; Pasupulety, L. *Langmuir* **2000**, *16*, 430.